OPTIMUM RIDGE LIFT A SCALED EXPERIMENTAL INVESTIGATION

by Edward F. Crawley and Michael Schmanske, Cambridge, MA (USA)

Presented at the XXIII OSTIV Congress, Borlänge, Sweden (1993)

Abstract

A series of scaled experiments were conducted to determine the optimum region of ridge lift for soaring flight. Two ridge models were placed in the MIT Wright Brothers' Wind Tunnel and tested under simulated atmospheric flow conditions, which included variations in incoming flow angle, ground roughness, and earth boundary layer. A five-hole Pitot-static probe was used to map the flow field to determine the region and intensity of maximum lift. Experimental data are presented, and correlated with a simple pilot-usable model.

Introduction

Soaring pilots use many natural sources of lift to keep their aircraft aloft, including mountain wave, thermal, and ridge lift. When in ridge lift, a sailplane takes advantage of the upward component of the air velocity as it moves over the upstream face of a ridge. Unfortunately for pilots, although long distance and competitive ridge flying have given rise to some heuristic rules concerning optimum flight zones, finding the maximum lift region is often a matter of an educated guess based solely on trial and error. This resembles the situation, before MacCready solved the optimum speed to fly problem [Ref. 6], when pilots had to estimate the best inter-thermal flight speed.

A simple and effective method for identifying the best region of ridge lift would be highly desirable. The objective of this work was to determine the location and intensity of optimum ridge lift under varying atmospheric and topological conditions, and to derive a pilot-usable model for extrapolating these results.

There is little detailed information about flow over a ridge as it pertains to soaring. In contrast, the flow over ground structures on ridges is documented in a number of sources [Refs. 1, 7]. Yet, while such research has produced numerous mathematical and computer simulations, little has been done to apply this knowledge for the benefit of soaring.

The classical soaring textbook model of ridge lift is highly simplified. It usually shows a sailplane flying upstream of a long straight semi-circular ridge with a completely smooth laminar flow impinging normal to the ridge [Ref. 5]. The motivation for this model is that the location of maximum lift can be easily derived from potential flow theory; it occurs along a line at 45 degrees to the vertical, with increasing intensity as the surface is approached. However, real ridges are not semi-circular or straight. The earth boundary layer and local surface roughness make naturally occurring atmospheric flow turbulent. And real flow is not necessarily normal to the ridge. Where then is a pilot to fly?

To address this question, a series of experiments were conducted on scaled models of straight and sinusoidal ridges with simulated cross-sections and surface roughness. Some tests were conducted with uniform inflow, and others with a simulation of the atmospheric boundary layer. The flow relative to the model could be pitched downward (to simulate the downwash of an upstream ridge or wave), and yawed sideways (to simulate flow at an angle to the ridge).

In the discussion below, the experimental procedure will first be outlined, followed by a presentation of the experimental results and their interpretation. Finally, a series of simple pilot-usable models are compared to the

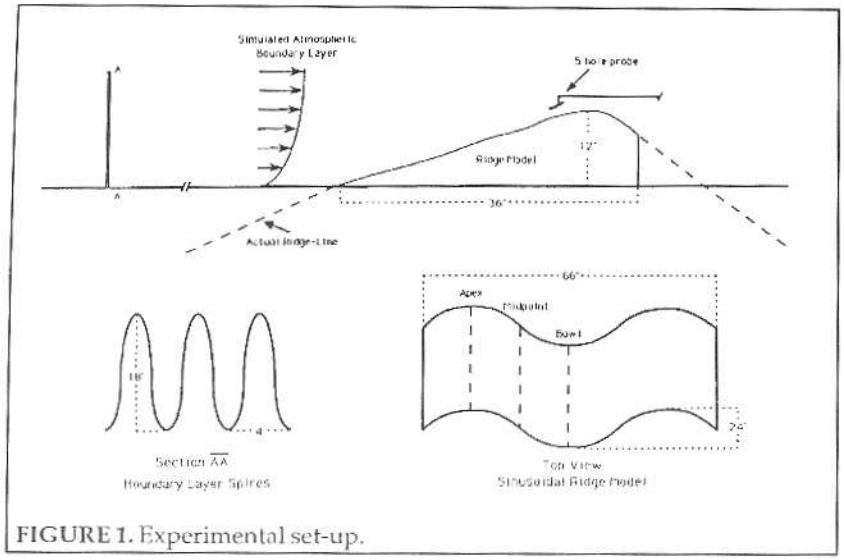

FIGURE 1. Experimental set-up.

data, and their usefulness as flying aids demonstrated.

Experiment Description

Ridge Models

Two ridge models were tested. The cross-sections of both were based on a north/south running ridge in the Green Mountains of central Vermont, located just to the east of the Sugarbush Airport and known officially as the Northfield Range. This ridge represents the extreme northern end of the Appalachian Mountain system which extends, with some interruptions, over 1200 miles from Maine to Georgia.

Three representative cross-sections were measured from topographical survey maps [Ref. 8], then averaged to create a representative section of the mountain ridge. As indicated in Figure 1, only the top 1200 feet were modeled, with a 1200:1 scale. This minimized wind tunnel test section blockage while retaining a scale large enough to allow accurate measurements in the critical flight zone.

The ridge models were 12 inches high and 48 inches long. The first 35 inches of the models consisted of the smooth windward upwards-sloping face. After the peak, the ridge models continued for another 13 inches, then dropped abruptly, leaving the leeward side incomplete. Flow measurements were taken only on the windward side. It was assumed that because the downwind slope was too steep to maintain attached flow, the effects of the abrupt termination would be masked in the separated flow region, and influence on the windward flow would be negligible. Before testing, this assumption was verified using flow visualization. Separation of the flow occurred approximately 6 inches after the ridge crest. This point was still 7 inches before the ridge dropped off abruptly. Flow visualization also indicated 2-dimensional flow for the cross-sections at which velocity profiles were measured.

Of the two models, the first was a straight ridge. As shown in Table 1, this model was used for all tests except those which examined curvature in the ridge line. For that non-ideal condition, a sinusoidal ridge was used, which possessed the same cross-section as the straight ridge model. If viewed from above, the amplitude of the sinusoidal nature of the ridge was 12 inches; i.e. 24 inches from the apex to the bowl.

In some tests, surface roughness on the upstream face was introduced. Soft rubber door mats were used to simulate the presence of ground clutter rocks and trees). Pliable enough to lay smoothly on the ridge without affecting the surface shape, the mats were also studded with nubs: cylindrical rubber protrusions 0.3 inches high and slightly less than 0.1 inches in diameter. These nub measurements simulated ground disturbances a little over 30 feet high and slightly less than 10 feet in diameter, each such 'tree' was spaced 0.25 inches (25 scale feet) from its nearest neighbor.

Inflow Conditions

The ridge models were placed on the floor turntable in the 7 by 11 foot test section of the MIT Wright Brothers' Wind Tunnel. In one test, 20 degrees of yaw (horizontal inflow angle from perpendicular) was introduced using the turntable. In another configuration, a tiltable platform enabled variations in pitch (vertical incidence angle) to simulate a 10 degree downward flow component onto the ridge. Such downwash could occur in the lee of another upstream ridge or mountain wave.

Testing was conducted at nearly standard temperature and pressure, and at an upstream air speed of 30

	Ridge			Inflow			
Test	Straight	Sine	Rough	Normal	20° yaw	10° down	Earth Bl.
1	X			X			
2	X					X	
3				X	X		
4	X		X	X			
5	X			X			X
6	X		X	X			X
7		X		X			
8		X		X			
9		X		X			

TABLE 1. Test Matrix

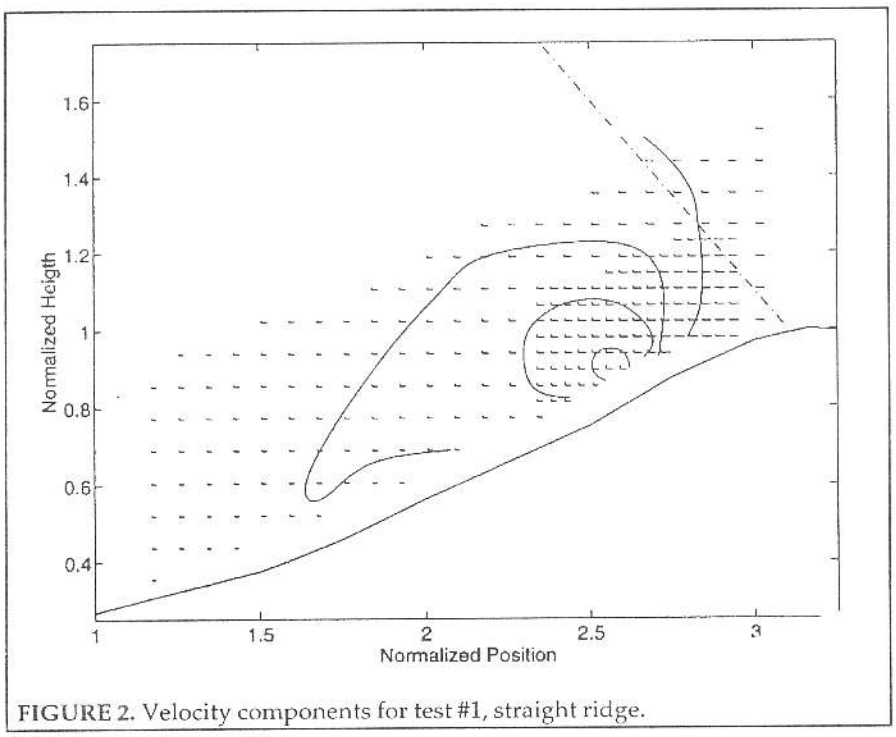

FIGURE 2. Velocity components for test #1, straight ridge.

miles per hour, producing a model Reynolds number of one million. The leading edge of the model was approximately 16 feet from the entrance to the test section. The nominal tunnel boundary layer was eliminated by raising the test platform 6 inches above the tunnel floor, placing the test section within near potential flow. No attempt was made to eliminate the nominal test section boundary layer, which had a thickness of .2 inches. In several tests, the influence of the atmospheric boundary layer was investigated. Boundary layer spires were used to simulate a 1:1200 scale one 1/6th power law boundary layer, typical of a fully developed turbulent boundary layer which evolves in a rural environment [Refs. 2, 3]. The 21 inch high spires were placed at the entrance to the test section, partially blocking the flow near the floor. Flow visualization confirmed that the flow had properly mixed when it reached the testing area, creating a smooth total pressure deficit resembling the deep atmospheric boundary layer.

Data Collection

All the data points for each test were taken at a fixed characteristic cross-section; for the tests on the straight ridge, this was the center of the model. For the sinusoidal ridge, data were taken at the maximum (apex), the minimum (bowl), and at a midpoint between the two.

The upstream velocity data were measured on a grid. The standard step size in both the vertical and axial direction was one inch. However, this was cut to half an inch near where it was believed maximum velocity would most likely lie, thus allowing both a larger scale view of the flow and higher resolution in the area of greatest interest.

A 5-hole Pitot-static tube was used for data collection. This type of Pitot tube measures both the vertical and horizontal angle of air flow, as well as the total and static pressure. Previous calibration found the probe to be accurate to within +/- 0.5 degree and 2% of free stream velocity [Ref. 4]. Using a Scani-valve, the data from the Pitot-static tube were sampled at 500 points over 5 seconds. Sampled data contained 0.1% RMS, indicating smooth flow conditions.

The 5-hole probe was suspended from behind by a long steel rod attached to an electronic traverse mechanism. The probe was tilted slightly down in pitch to allow measurements closer to the ridge and insure the body of the probe was more closely aligned with the mean flow in the measurement region.

Probe output measurements were converted into pressure coefficients. Alpha (vertical flow angle, pitch), beta (horizontal flow angle, yaw) and relative velocity

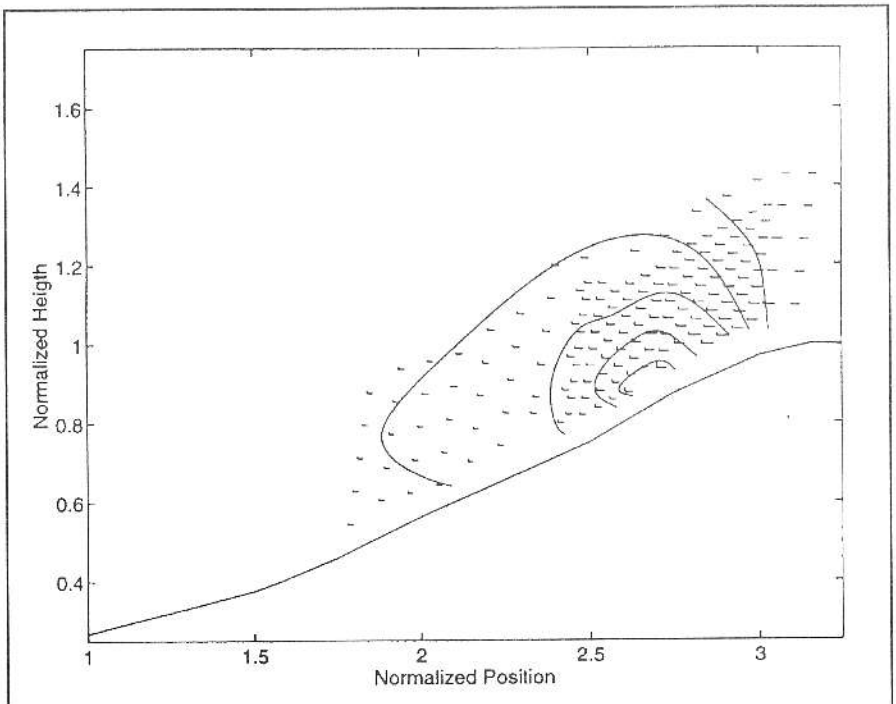

FIGURE 3. Velocity components for test #2, incoming flow 10 degree down pitch.

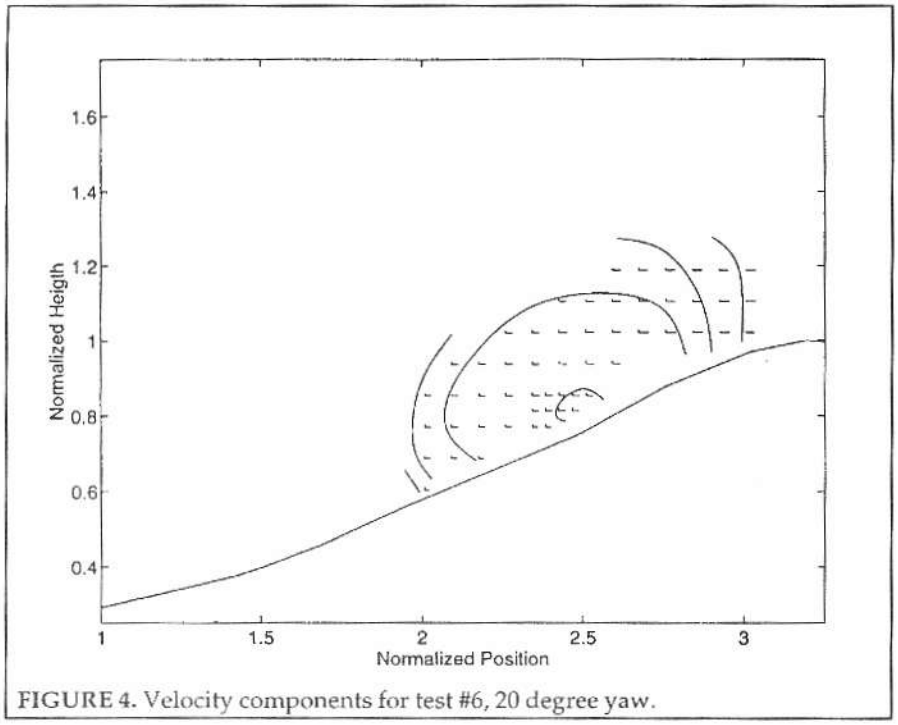

FIGURE 4. Velocity components for test #6, 20 degree yaw.

were then calculated. After correcting alpha by the probe inclination, the vertical and horizontal velocities were computed, and are shown on the figures of the next section.

Experimental Results

Test Matrix

With four possible measurement sections (one on the straight ridge, and three on the sinusoidal ridge), two yaw angle, two pitch angles, local surface roughness and earth boundary layer options, 64 tests could have been conducted. The nine tests in Table 1 were selected to cut across the principal axes of this test matrix. As testing progressed, a smaller area was scanned to locate and document the optimum conditions.

Straight Ridge

The velocity profiles for the straight ridge tests are shown in Figures 2-7, first for the baseline test (Figure 2), then for the changes in inflow angle (Figures 3 and 4), and finally for the variations in inflow boundary layer profile (Figures 5-7).

The results of the baseline test (Figure 2) show how the flow would accelerate up a ridge in the case of a normal flow and a very thin earth boundary layer (recall that the test section boundary layer was not removed). This is the closest approximation in these tests to the simple ridge flow model found in classical soaring texts. The components of the axial and vertical flow are shown separately, and are normalized by the far upstream inflow velocity. The axial component of the flow and the total velocity accelerate uniformly from the leading edge of the ridge to the peak. This is consistent with a venturri-like acceleration due to the local potential contraction of the streamlines. The vertical component of the flow (the one of primary interest to soaring pilots) is indicated by the contours drawn on Figures 2-7. The maximum vertical velocity component occurs well before the peak, and has a value of 0.26. For reference, an unaccelerated flow turning parallel to a grade of 12/35 would develop a vertical component of 0.32. Clearly, some combination of incomplete turning and flow deceleration in the boundary layer prevents this value from being attained.

It is interesting to note that the maximum total velocity and the maximum vertical velocity do not occur at the same point. The total velocity of the flow increases as it progresses toward the peak, due to potential flow contraction. Close to the model, the angle of the flow approaches the angle of the ridge surface. From these two observations, it can be inferred that the maximum vertical velocity component occurs at a point possessing the greatest product of the ridge slope and the total

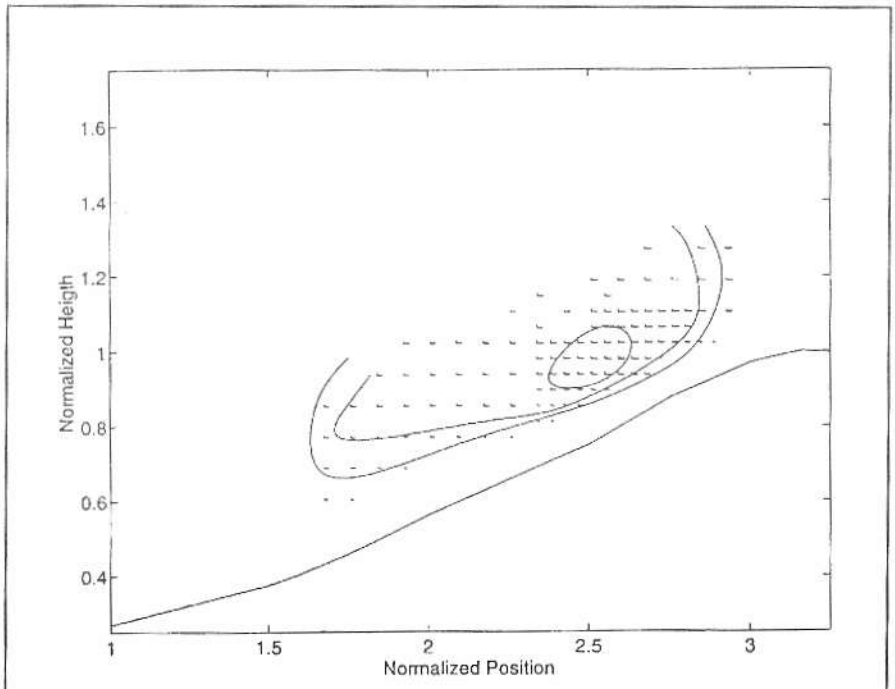

FIGURE 5. Velocity components for test #3, surface roughness.

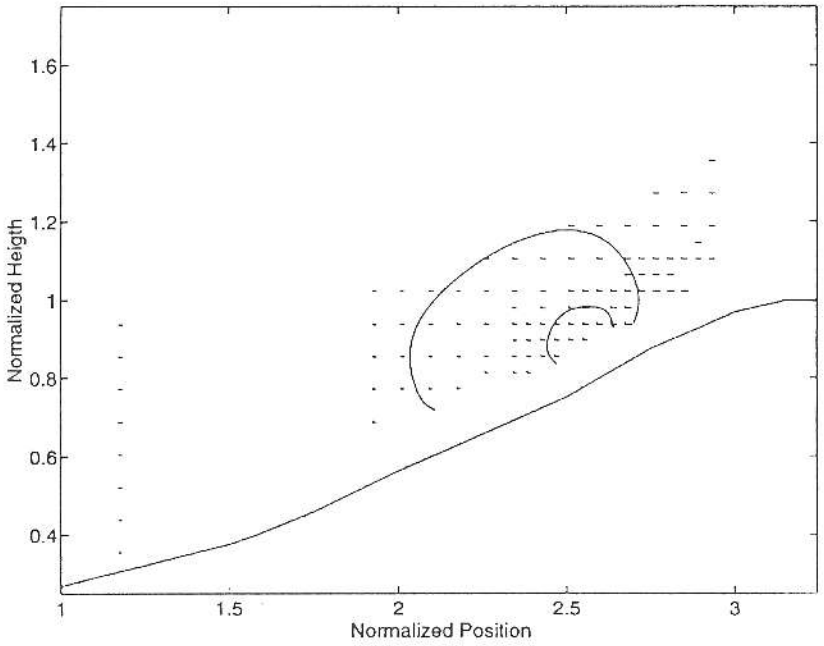

FIGURE 6. Velocity components for test #4, boundary layer.

velocity.

Such a region occurs well before and below the ridge peak. However, it is lower, further from the peak, and more compact than would be inferred from common ridge soaring practice. The line along which a novice ridge pilot might fly, running at 45 degrees from the peak, passes through areas of significantly weaker lift. In fact, while flying along this line, soaring conditions do not uniformly strengthen as the pilot approaches the ridge. This explains in part why superior ridge pilots are often observed "down low on the trees."

Changes in pitch and yaw inflow angles modify these observations slightly. Downflow onto the ridge, which might be thought to harm ridge flying, actually helps. The approximate shapes of the vertical velocity contours in Figure 3 are much the same as in Figure 2. However, the area of high vertical velocity is larger, and the peak measured vertical velocity is actually 0.32. The presence of the downflow has thinned the boundary layer, allowing a more potential-like flow closer to the surface. This would suggest that it is not regions of downwash from preceding ridges which should be feared by the ridge pilot, but perhaps regions of upwash, which would tend to lift and thicken the earth boundary layer.

The introduction of inflow yawed to the line of the ridge changes the contours more dramatically, as seen in Figure 4. Compared to the baseline of Figure 2, the region of maximum vertical velocity has enlarged and extended downhill. The maximum measured vertical velocity is now 0.28. Two factors are at work here. From the perspective of the potential flow, only the component normal to the ridge will be affected. However, with only 20 degrees of yaw in the inflow, this change is not sufficient to explain the differences between Figures 2 and 4. From the perspective of the viscous effects, the flow traverses the ridge a longer distance, allowing thickening of the boundary layer compared to the normal flow. Both potential and viscous factors contribute to a larger, less intense zone of ridge lift.

The inclusion of forest-like surface roughness (Figure 5) tends to raise the area of maximum vertical velocity upward away from the ridge. A local boundary layer forms due to the roughness, which slows the flow close to the ridge. Since total velocity in general decreases with distance from the model, this lowers the value of the maximum vertical velocity to 0.21.

The test with an earth atmospheric boundary layer (Figure 6) indicates a general slowing of the flow throughout the ridge soaring area. While this reduces the vertical velocity maximum to 0.17 (or 65% of the value in the

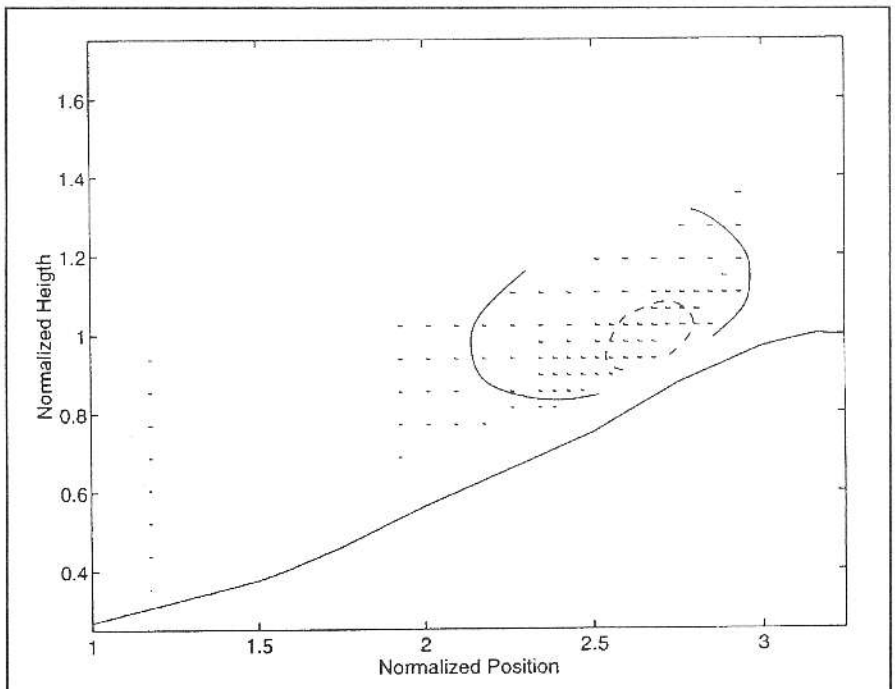

FIGURE 7. Velocity components for test #5, surface roughness and boundary layer.

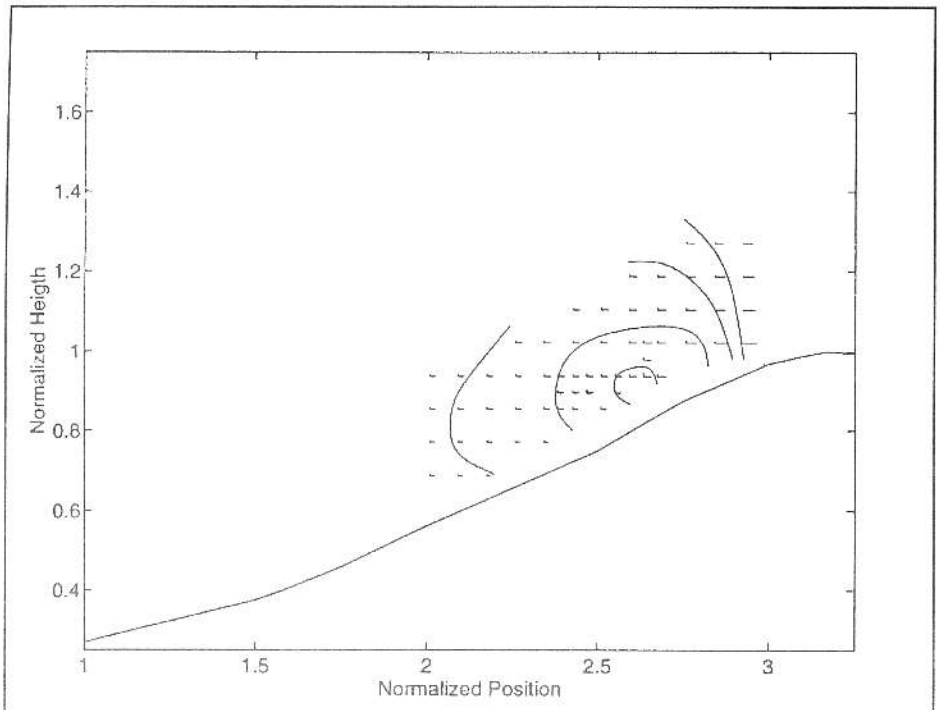

FIGURE 8. Velocity components for test #7, sinusoidal ridge, apex.

baseline test of Figure 2), it had little effect on the location of the maximum or on the distribution of vertical velocity in the ridge soaring area. These changes are due to the fact that the earth boundary layer has a scale height comparable to the ridge. In effect, in this test the ridge operates within the earth boundary layer in normal conditions.

The most realistic case is shown in Figure 7, which includes both surface roughness and atmospheric boundary layer. By comparison with Figures 5 and 6, the additive effects of the lifting of the local boundary layer and weakening due to the atmospheric boundary layers are both apparent. Unfortunately, the peak vertical velocity has diminished to 0.14. For a fixed inflow velocity, increasing realism leads to weaker ridge lift.

Sinusoidal Ridge

Measurements were taken at three positions on the sinusoidal ridge: the apex, midpoint, and bowl of the ridge. The flow behavior observed at the apex of the ridge (Figure 8) was nearly identical to the baseline straight ridge (Figure 2). The maximum vertical velocity was 0.26, identical to that of the straight ridge. The transverse flow was extremely small, as would be expected for a symmetric blunt protrusion into the flow.

The vertical velocity values for the cross-section taken at a midpoint between the apex and the bowl were also quite comparable to a straight ridge (Figure 9), although the zone of maximum lift had been extended slightly up the ridge. The actual maximum value of vertical velocity remained 0.26. The transverse flow measurements taken at this point indicated a small but measurable channeling of the flow toward the bowl of the ridge.

The bowl (or valley) of the ridge exhibited the most interesting vertical velocity distribution. The lower side of the maximum vertical velocity zone began at approximately the same level as the previous tests. However, the size of the zone had 'stretched' up the ridge much farther than in the other tests, so that the uphill contour was nearer the peak. There was one measured point of vertical velocity of 0.29, but the next highest two points were 0.25 and 0.24, indicating that on average the effect of the bowl was not to intensify the vertical velocity, but to raise the location of the maximum closer to the top of the ridge.

The result of this shift was that the lift along the 45

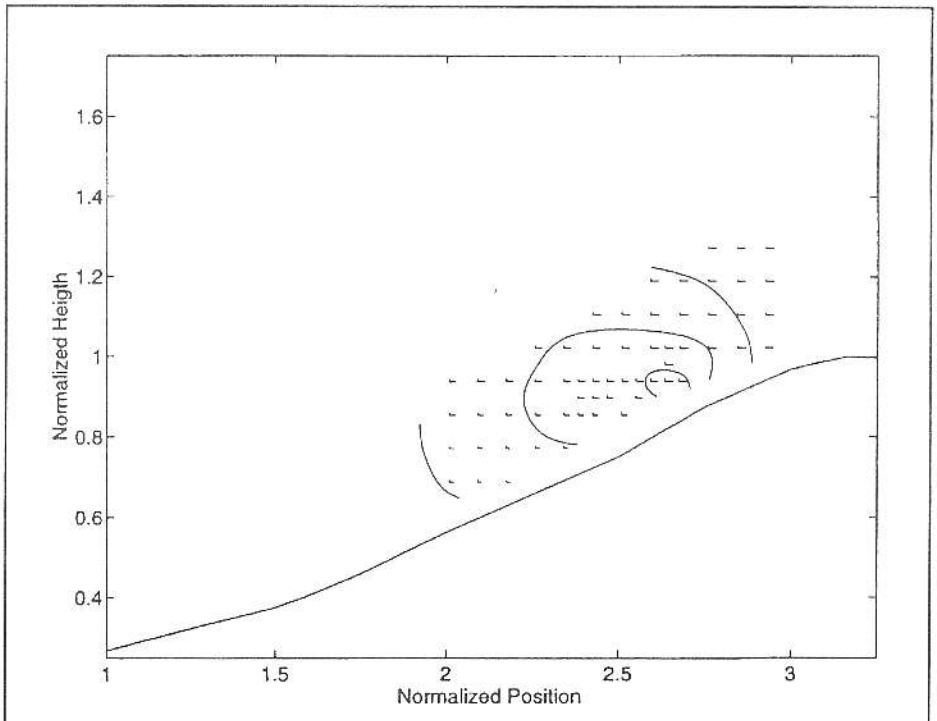

FIGURE 9. Velocity components for test #8, sinusoidal ridge, midpoint.

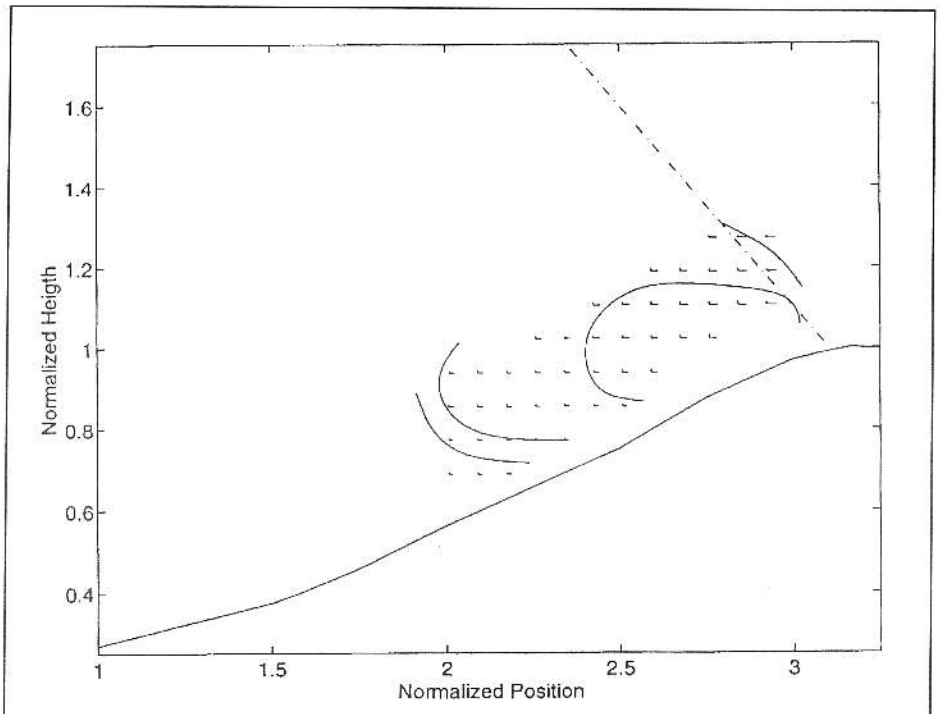

FIGURE 10. Velocity components for test #9, sinusoidal ridge, minimum.

degree line from the peak (the line which might be flown by a novice) had strengthened significantly. Comparing Figure 2 for the straight ridge and Figure 10 for the bowl of the ridge, the apparent maximum vertical velocity along this line increased by a factor of two. This can be perceived as a strengthening of the ridge lift in the bowl, even though it was not the magnitude but the location of the maximum lift which had changed. Further, the ridge lift would uniformly increase with decreased altitude, allowing the pilot to feel more comfortable flying close to the ridge.

Model Correlation

The objective of model correlation is to create a simple, physically-based model which can be correlated with the data and used by a pilot in flight. The problem with the traditional semi-circular ridge model is that it yields the guidance to fly at 45 degrees upstream of the hill, but with no underlying physical insight as to how to approach a real ridge.

For the half-cylinder in potential flow, two effects are at work. The total velocity increases with height on the surface, due to streamline contraction, and reaches a maximum at the peak. Near to the 'ridge,' the flow angle matches the angle of the surface of the cylinder, starting at a maximum at the base of the 'ridge,' and reaching zero at the peak. The maximum vertical velocity occurs at a point where the product of the total velocity (increasing with height) and the slope (decreasing with height) is a maximum. For a simple inviscid semi-circle, this is at 45 degrees, or exactly midway between the base and the peak. This physical insight (that the maximum vertical velocity occurs at the point where the product of slope and total velocity is a maximum) is used to fit a mathematical model to the experimental results.

To derive a quantitative comparison, a 'flying height' is defined at 150 scale feet (1.5 inches) above the ridge. While this is higher than many glider pilots fly, it is the lowest altitude for which there are consistent data available from all tests. As an example, the measured vertical velocity at this flying height as a function of distance from the leading edge of the ridge is shown in Figure 11 for the baseline straight ridge test.

Several models are correlated with the data. All involve a product of the local slope with an estimated

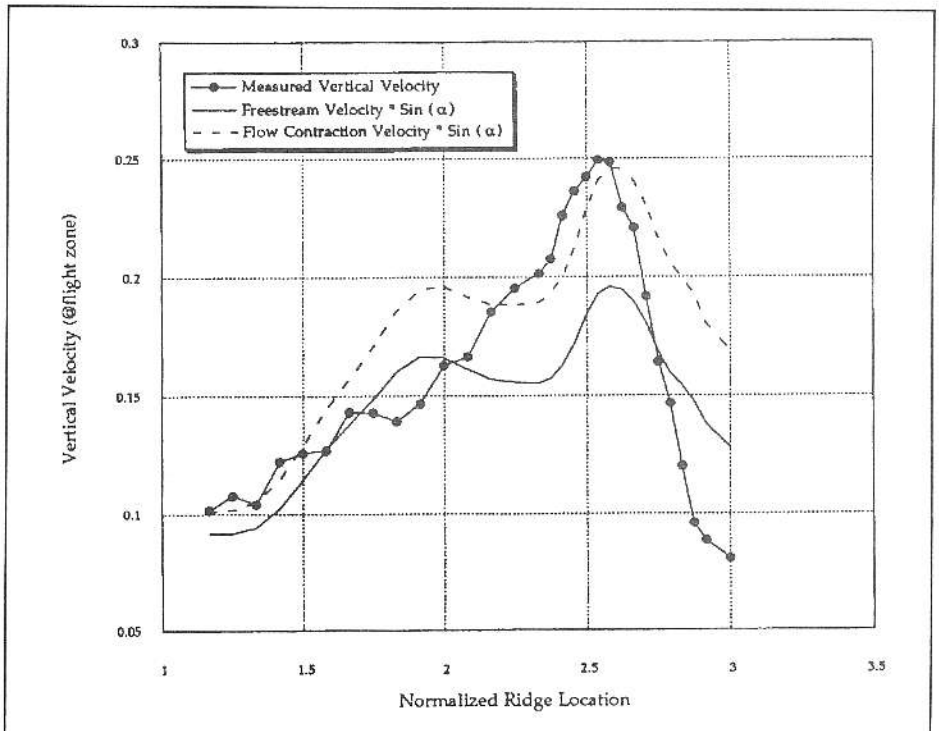

FIGURE 11. Vertical velocity analytical predictions.

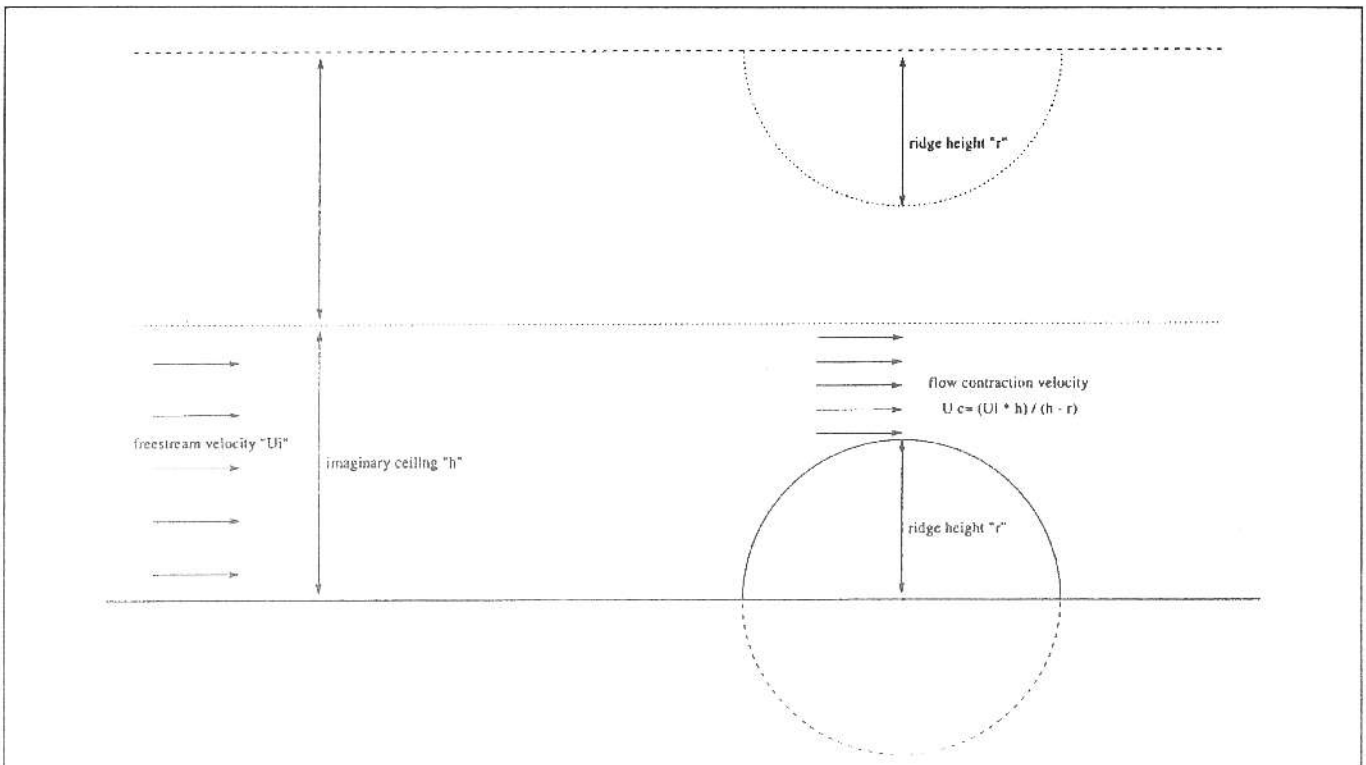

FIGURE 12. Flow contraction around a semi-circular ridge in two-dimensional potential flow.

velocity. The simplest model, shown by the solid line in Figure 11, forms the product of the free-stream velocity (as measured by a single upstream Pitot-static tube) times the sine of the ridge angle at the point in question. This model accurately predicts the location of the maximum at the horizontal coordinate of 2.6, but does not accurately predict the magnitude of the velocity. Obviously, this model does not capture the contraction-induced acceleration of the flow over the ridge.

An accurate model of the flow acceleration would of course require a potential solution of the outer inviscid semi-infinite flow field, useful in experimental data correlation, but meaningless as a pilot-usable model in the cockpit.

As motivation for a simpler contraction model, consider once again the simple semi-circular ridge. For such a case, the flow velocity at the top of the half-cylinder equals twice the free-stream velocity. The flow acceleration in the vicinity of the ridge can be closely approximated by imagining the ridge and its reflection about an image line to form a channel or nozzle, as shown in Figure 12. By placing an image plane at twice the height of the ridge, the solution that the total velocity at the top of the cylinder equals twice the freestream velocity entering the 'nozzle' is recovered.

To apply this model to flow over the ridge, one imagines an image plane or 'invisible ceiling' placed at some height above the top of the ridge. By changing the height of this 'ceiling' one can change the ratio by which the free-stream velocity entering the ridge 'nozzle' is multiplied. Figure 11 shows the correlation of this model with the measured data for the straight ridge, assuming an image plane 30 inches above the ridge top. Note that now both the magnitude and location of the zone of maximum vertical velocity are predicted accurately.

To use this model while piloting a sailplane, one would first imagine the airflow over the ridge as incompressible flow in a channel with a half-height of 3.5 to 4 times the ridge height. Then one would estimate the flow acceleration in this hypothetical channel and assume local flow is approximately parallel to the slope of the ridge. By taking the product of the estimated flow velocity and the local slope, one can determine the most likely area of maximum lift.

Conclusions

Based on the experimental data, the following observations can be made regarding the flow over smoothly contoured straight ridges:

The total velocity increases towards the peak due to potential flow contraction and is tangent to the surface near the ridge. As a result, the maximum total velocity and vertical velocity do not occur at the same point.

The maximum vertical velocity occurs when the product of the slope times total velocity is greatest. For a smooth ridge, this is well below and before the peak. This implies optimal ridge soaring occurs at a location quite different than suggested by classical texts.

Downwash on a ridge due to upstream hills can

intensify the ridge lift by thinning the boundary layer and therefore creating a higher local upward vertical velocity.

Small amounts of cross flow, due to the wind striking the ridge at a small angle, do not appear to weaken the ridge lift, and may slightly enlarge the region of optimum flying.

The presence of surface roughness in the form of trees or rough terrain thickens the local boundary layer, and tends to slightly weaken the lift and to raise the region of maximum lift up off of the surface of the ridge.

The presence of a well developed earth boundary layer whose scale height is equal to or greater than the height of the ridge weakens the lift considerably, but does not change the location of the region of maximum lift.

The following observations can be made regarding the flow over smoothly contoured curved ridges:

The vertical velocity distribution at the apex of the ridge is very similar to that for a straight ridge.

The maximum vertical velocity in the bowl is only slightly larger than at the apex. The primary effect of the bowl is not to straighten the lift, but to raise the area of maximum lift up towards the peak.

A pilot-usable model correlates well with the data and predicts the location and strength of the maximum lift. To use this model, the pilot estimates the flow acceleration, and flies where the product of flow acceleration and slope is greatest. This will almost always be well below and in front of the peak. For significant surface roughness, the estimate of the optimum altitude should be adjusted upward.

The overall conclusion of this work is that the world's best ridge pilots have, by trial and error, discovered and internalized the models for locating maximum ridge lift. These observations are now placed on a firmer theoretical basis. This approach to guidance is quite different from that found in basic texts on soaring, and is now available for all to investigate in their own full-scale experiments.

Acknowledgments

The authors would like to acknowledge the experimental contributions of Carrie Allen and Hank Sawtelle, who conducted an earlier investigation with these ridge models, and of Donald S. DeLong, who collected the data presented here.

References

1. Bowen, A.J., "The Prediction of Mean Wind Speeds Above Simple 2D Hill Shapes," Journal of Wind Engineering and Industrial Dynamics, 15 (1983), Elsevier Science Publishers, B.V., Amsterdam, pp. 259-270.
2. Counihan, J., "Adiabatic Atmospheric Boundary Layers: A Review and Analysis of Data from the Period 1880-1972," Atmospheric Environment, Pergamon Press, Vol. 9, 1975.
3. Davenport, A.G., Isyumon, N., "The Application of the Boundary Layer Wind Tunnel to the Prediction of Wind Loading," Proceedings of the International Conference on Wind Effects on Buildings and Structures, Vol. 1, Ottawa, Canada, Sept. 1967.
4. Dwyer, W.P., "Measurement of Flow Boundary Condition Data and Wing Pressures in a Wind Tunnel Test of a 45 Degree Swept Wing," Master of Science Degree Thesis, Massachusettes Institue of Technology, Feb. 1990.
5. Reichmann, H., *Cross-Country Soaring*, Thomson Publications, Santa Monica, CA, 1978.
6. Reichmann, H., *Flying Sailplanes*, Thomson Publications, Santa Monica, CA, 1980, pp. 96-97.
7. Teunissen, H.W., Shokr, M.E., "Wind Tunnel/Full Scale Comparisons of Boundary-Layer Flow over Askervein Hill, Scotland," Asia Pacific Symposium on Wind Engineering, University of Roorke, Roorke, India, Dec. 5-7, 1985, pp. 8794.
8. United States Geological Service chart, DMAG472IINW-Series V8 13, 1980.